Title: Temperature fractionation, physicochemical and rheological analysis of psyllium seed husk heteroxylan

Author names and affiliations
Yi Ren[1] yi.ren@nottingham.ac.uk +44(0)1159516012
Gleb E. Yakubov[1] sbzgy1@exmail.nottingham.ac.uk
Bruce R. Linter[2] Bruce.Linter@pepsico.com
William MacNaughtan[1] sczbim@exmail.nottingham.ac.uk
Tim J. Foster[1] Tim.Foster@nottingham.ac.uk

[1] Division of Food Sciences, School of Biosciences, University of Nottingham, Sutton Bonington Campus, Loughborough, LE12 5RD, UK
[2] PepsiCo International Ltd, 4 Leycroft Rd, Leicester, LE4 1ET, UK

Highlights:

- Psyllium husk heteroxylan is fractionated by a straightforward method
- Fractions show distinct rheological properties
- Arabinose/xylose ratio can be estimated by 2nd-derivative FTIR and ^{13}C NMR spectra
- Composition and spatial arrangement of sidechains are influential
- Two hypotheses were proposed

Keywords:

Psyllium husk, Heteroxylan (arabinoxylan), Time-temperature superposition (TTS), Temperature fractionation, arabinose/xylose ratio, rheology

Abstract

Psyllium husk is a source of natural dietary fibre with marked water absorbability and gelling properties, which makes it an attractive functional ingredient for applications in the food industry, such as gluten free bread and breakfast cereals. The main functional component of psyllium husk is a complex branched heteroxylan. In this study, a straightforward sequential fractionation of hydrated psyllium seed husk powder based on temperature-dependent behaviours was applied. The F20 (20°C fraction) showed the highest yield followed by F60 while 13.5% of the husk is unextractable (residue).

The obtained fractions showed unique rheological properties as analysed using small amplitude oscillatory shear rheometry and the time-temperature superposition (TTS) technique. The results indicate that: 1) only F20 was influenced by heat treatment, 2) high temperature fractions showed stronger gel properties, 3) a three-step softening/melting was observed, 4) F60 has longest relaxation time as shown in TTS master curves. The four fractions were also characterised using the monosaccharide analysis, FTIR and ^{13}C NMR. The arabinose/xylose ratio was found to increase with the increase in fractionation temperature. FTIR and ^{13}C-NMR spectra supported that low temperature fraction is less branched.

Two hypotheses were therefore proposed: The first one based on models by Haque, Richardson, Morris and Dea (1993) and Yu et al. (2019) focusing on chemical and structural properties of the molecules. The second hypothesis highlights differences in hierarchical molecular conformations of polysaccharides which is proposed by Diener et al. (2019). Sidechain substitution and composition and length of sidechains are critical and significantly influence the properties of each fraction.

1. Introduction

Psyllium, also known as ispaghula or isabgol, refers to *Plantago ovata* Forsk. Its seed husk is a source of natural dietary fibre, which has good water absorbability and shows gelling properties and can, therefore, be applied in food production as a novel functional ingredient. Psyllium has been being traditionally used in medical treatment in some countries and it is proven that psyllium has the ability to lower cholesterol levels, be used as laxative, and improve insulin sensitivity (Anderson et al., 2000; Madgulkar, Rao & Warrier, 2015; Song, Sawamura, Ikeda, Igawa & Yamori, 2000). Psyllium seed husk is currently widely used in applications ranging from gluten free bread making to drug delivery thanks to its high water binding capacity, thickening effect and gel-forming ability (Cappa, Lucisano & Mariotti, 2013; Chavanpatil, Jain, Chaudhari, Shear & Vavia, 2006; Haque & Morris, 1994; Mancebo, San Miguel, Martínez & Gómez, 2015; Mariotti, Lucisano, Pagani & Ng, 2009; Singh, 2007).

The functional part is the mucilage from the seed husk where the main polysaccharide is heteroxylan mainly composed of (1 → 4) linked β-D-xylose with sidechains on C-3 or C-2 positions containing arabinose and xylose in various motifs (Edwards, Chaplin, Blackwood & Dettmar, 2003; Fischer et al., 2004; Guo, Cui, Wangb & Young, 2008; Yu et al., 2017). Small amounts of galacturonic acid and rhamnose were also identified and other reports stated that the psyllium seed husk heteroxylan is slightly charged (Fischer et al., 2004; Guo, Cui, Wang, Goff & Smith, 2009; Guo et al., 2008; Yu et al., 2017). Laidlaw and Percival (1949) evidenced that extracts of psyllium seed husk contain both neutral arabinoxylan(heteroxylan) and polyuronide, however, Farahnaky, Askari, Majzoobi and Mesbahi (2010) reported the presence of carboxylic groups on the heteroxylan molecules. However, Fischer et al. (2004) found that the main compound, arabinoxylan, is neutral but with trace amounts of other sugars. The conflicts in full agreement of structure often lie in different extraction methods adopted.

Most studies on the psyllium husk are based on defined extraction and sometimes fractionation methods. Farahnaky et al. (2010) mechanically extracted psyllium husk heteroxylan with water with a yield of 28.5%. However, alkaline extraction is more common. Guo et al. (2008) extracted and fractionated psyllium gums by hot water and alkaline solutions with yield up to 61.4% for an alkaline gel fraction and the molecules in different fractions showed different molecular structures and stability in terms of hydrodynamic radius.

Marlett and Fischer (2005) and Fischer et al. (2004) used alkaline and acid solutions to extract and fractionate psyllium husk heteroxylan (highest yield is 57.5% for alkaline extracted gel) and they also showed differences on the molecular composition and viscosity. More information about extractability of psyllium husk polysaccharide was recorded by Van Craeyveld, Delcour and Courtin (2009) showing an extraction increase being more significant when the concentration decreased rather than with a temperature increase, showing effects on gel structure. They also observed a higher yield using an alkaline extraction method, where the charge state of uronic acid is affected.

Although psyllium husk polysaccharide has been extracted and fractionated by water and alkaline solutions and the fractions show differences in terms of molecular structure and rheological properties, they all show gel-like property when hydrated in water (Farahnaky et al., 2010; Guo et al., 2009; Haque et al., 1993; Yu et al., 2017). An earlier study by Haque et al. (1993) proposed a 'weak gel' property describing the rheological behaviour of the psyllium husk polysaccharide dispersion. Guo et al. (2009) investigated the structure and rheological properties the gels of alkaline extracted psyllium husk heteroxylans and the subsequent influence of Ca^{2+}. They found that the addition of Ca^{2+} changed the gel microstructure from fibres to aggregates, increased elastic modulus and critical strain in a certain range of addition levels, and increased thermal stability. The influences of concentration, temperature, and pH on the gel properties were investigated by Farahnaky et al. (2010). They found that freeze-dried psyllium gel adopts lath sheet-like structure, and higher concentration, heat treatment, and higher pH increased structure stability, generated ordered structure, and decreased pore size distribution respectively. Efforts have also been made to modify the properties of psyllium husk polysaccharides by acid treatment and phosphorylation (Cheng, Blackford, Wang & Yu, 2009; Rao, Warrier, Gaikwad & Shevate, 2016). For the mechanism of the gel-like property, an early study attributed gelation to the association of unsubstituted $(1 \rightarrow 4)$ linked xylan backbones existing as continuous blocks (Sandhu, Hudson & Kennedy, 1981). Later Haque et al. (1993) described the polysaccharides as being packed as strands which then form a 'weak gel' with tenuous interactions. The latest work has focused on the stability and importance of hydrogen bonds between sidechains maintaining and influencing the gel structure and property (Yu et al., 2019).

Because psyllium husk powder is usually applied as dispersion in water, whose property is influenced by temperature, and, given that different structures have been observed in the whole psyllium husk powder dispersion, this study extracted and fractionated psyllium husk dispersion in water at different temperatures by a straight, simple, and sequential process which can be easily applied in industry to generate fractions with different rheological properties. Additionally, exploring the chemical and molecular structures, conformations and microstructures provided a better understanding of the mechanism of the gel-like rheological property. Psyllium husk polysaccharide is widely referred to arabinoxylan in the literature due to the high content of arabinose and comparability to other arabinoxylan found in other cereal materials and hemicellulose. However, 'heteroxylan' is adopted in this work because of the complex sidechains.

2. Methods and materials

2.1. Materials

Psyllium husk powder (Vitacel®) was kindly donated by the JRS (J. Rettenmaier & Söhne Group, Rosenberg, Germany). Toluidine blue and methyl blue was purchased from Sigma–Aldrich (UK).

2.2. Temperature fractionation and sample preparation

The psyllium husk polysaccharides were extracted and fractionated in the water at 20 °C, 40 °C, 60 °C, 80 °C and 100 °C which are labelled F20, F40, F60, F80 and F100. The unextractable polysaccharides and other unidentified substances are residue. More specifically, 10 g of psyllium husk powder were hydrated in 2000 ml of reverse osmosis (RO) water for 2 hours with stirring and then homogenized by an Ultra-Turrax homogenizer (T25, Ika®-Werke, Germany) for 10 min. The dispersion was then centrifuged (Beckman J2-21 centrifuge, rotor JA-10) at 17700 g and 20 °C for 60 minutes. The supernatant was collected and freeze-dried and labelled as F20. The gel and insoluble phases were redispersed to the volume of 2000 ml by high speed shearing for 1 minute using an Ultra turrax homogeniser and then 2 hours stirring at 40 °C. The dispersion was homogenised for 10 minutes again and centrifuged at 17700 g and 40 °C for 60 minutes. The supernatant was collected and freeze-dried and labelled as F40. The same procedure was performed on the remaining gel and solid part but at 60 °C, 80 °C and 100 °C. The supernatants of high temperature fractions were

concentrated by rotary evaporator with the temperature set at 60 °C to facility freeze drying. The residue was also freeze dried.

The yields of different temperature fractions are shown in Table 1. The highest yield is observed for F20 with F100 having the lowest yield. The yield of residue is slightly higher than that observed by Guo et al. (2008). They reported that some water-extractable heteroxylan is trapped within the husk walls and can be released only under alkaline conditions. Therefore, the conditions used in this study, i.e. 100 °C and high shearing, is not sufficient to fully extract the psyllium husk polysaccharide.

For rheological and other tests, a fresh dispersion was prepared by dispersing psyllium husk powder in RO water and allowed to hydrate for 1 hour at room temperature before tests. F20 was dispersed using an Ultra turrax in water and hydrated at room temperature for 30 minutes with stirring. The sample was degassed under vacuum and stirred for another 30 minutes. F40, F60 and F80 were prepared in a similar way and stirred at corresponding temperatures. Stock dispersions were prepared in the same way and stored at 4 °C.

2.3. Chemical composition and monosaccharide analysis

The protein content of psyllium husk powder was converted with the factor of 6.25 from nitrogen content analysis by Nitrogen Analyser NA 2000 (Fisons Scientific Equipment, Loughborough, UK). Lipid content was obtained by extraction with a chloroform-methanol mixture (2:1). Moisture content was obtained by drying at 105 °C and ash content was measured by a muffle furnace at 550° for 6 hours.

Monosaccharide composition of whole psyllium husk powder and fractions were analysed by hydrolysing 2 mg of samples in 66.7 µl 12M sulphuric acid for 1 hour at 37 °C followed by incubation at 99 °C for 2 hours after dilution to 1M sulphuric acid. The supernatants were then diluted 100 times with 10mM NaOH. Analysis of monosaccharides was performed by high-performance anion-exchange chromatography with pulsed amperometric detection (HPAEC-PAD) (Dionex, UK) with a CarboPac PA20 column. The mobile phase was 10mM NaOH with a flow rate of 0.5 ml min^{-1}. The data were calculated against arabinose, galactose, glucose and xylose as standards.

2.4. ATR-FTIR measurements

FTIR spectra of whole psyllium husk powder and freeze-dried fractions were collected by a Bruker Tensor 27 spectrometer (Germany) equipped with diamond attenuated total reflection (ATR) crystal in the range from 4000 to 550 cm^{-1}. The spectra were acquired averaging 128 scans with a resolution of 4 cm^{-1} against an empty background. Normalisation and baseline correction on whole spectra were performed by Opus 7.2.139.1294. Smoothing and 2nd derivatives of spectra over 1020 to 920 cm^{-1} were calculated by GraphPad Prism 7.04.

2.5. ^{13}C solid-state Nuclear Magnetic Resonance (^{13}C CPMAS NMR)

Carbon-13 cross-polarization magic angle spinning nuclear magnetic resonance (^{13}C CPMAS NMR) spectra of dry samples were recorded on a Bruker AVANCE III 600 NMR spectrometer (Karlsruhe Germany) equipped with narrow bore magnet and 4-mm triple resonance probe. Samples were packed into 4 mm rotors and spun at 10 kHz. Adamantane with an upfield peak (29.5 ppm) was tested as an external standard to reference chemical shift scales. The Proton 90° pulse length was 3 μs followed by contact period with 83 kHz for field strength of the proton and spin locking field.

Peak fitting was performed on certain peaks by Lorentzian function as shown in equation (1) where y_0, x_c, w and A indicate baseline, peak centre, peak width at half maximum and area under the peak respectively. The areas were used to estimate A/X ratio.

$$y = y_0 + \frac{2A}{\pi}\frac{w}{4(x - x_c)^2 + w^2} \qquad (1)$$

2.6. Rheological properties

Oscillation tests were performed using an MRC 301 rheometer (Anton Paar, Austria), with parallel plate geometry including a Sandblasted upper plate (PP50-SN11649, Anton Paar). The measuring gap was 1 mm. Extra sample was trimmed by a spatula and the edge of samples was covered by low viscosity mineral oil (Sigma, USA) to prevent drying of samples. The temperature was controlled by a Peltier system with the assistant of a water bath (R1, Grant, Shepreth). Amplitude sweeps, frequency sweeps, temperature sweeps and time dependence tests were performed.

147 The freshly prepared dispersion of psyllium husk powder was tested at both 20 °C and 98 °C.
148 The tests at 98 °C were performed by loading a sample at room temperature, increasing to
149 98 °C, and holding for 500 seconds before tests. Tests on heated and cooled samples were
150 performed by loading samples at room temperature, increasing to 98 °C, holding for 10
151 minutes, cooling back to 20 °C, and holding for 120 seconds before tests. During temperature
152 sweep tests, the temperature was increased from 20 °C to 98 °C, held for 10 minutes, and
153 cooled back to 20 °C. The heating rate was 1 °C min^{-1}. Two cycles of heating and cooling
154 were applied to psyllium husk powder dispersion with 2 hours holding at 20 °C in between.

155 For the fractions, freshly prepared samples were loaded onto the rheometer at 20 °C. F20 was
156 first subjected to a frequency sweep test at 20 °C followed by temperature sweep tests with
157 the same temperature profile for the whole psyllium husk powder sample as described above.
158 A frequency sweep test was performed again after the end of the second heating and cooling
159 circle followed by an amplitude sweep test. F40, F60 and F80 were also loaded at 20 °C but
160 the temperature increased to 40 °C, 60 °C and 80 °C individually and frequency sweep tests
161 were performed at corresponding temperatures. The samples were cooled back to 20 °C and
162 the same sequence of tests on F20 were performed. Samples rested for 120 to 500 seconds
163 before tests and between two different tests. Amplitude sweep tests were performed at a
164 frequency of 10 rad s^{-1} and frequency tests were performed with a strain of 0.2% which is in
165 the linear viscoelastic (LVE) region. Strain and angular frequency applied in temperature
166 sweep tests were 0.2% and 10 rad s^{-1} respectively.

167 To perform time-temperature superposition (TTS), the mechanical spectra of 4 fractions were
168 obtained at different temperatures ranging from 20 °C to 80 °C. More specifically, the sample
169 was loaded at 20 °C and the temperature changed in the range from 20 °C to 80 °C during
170 which the sample was tested at each constant temperature. The tests at each temperature were
171 repeated at least twice ignoring the temperature history ahead. The strain used at low
172 temperatures was 0.2% but it was 2% at temperatures higher than 60 °C to reduce noise.

173 **2.7. Fluorescence and optical microscopy**

174 Psyllium husk powder was dispersed and hydrated in an aqueous solution of 0.1% toluidine
175 blue for 1 hour. A drop of the dispersion was mounted onto the hot stage (THMS600,
176 Linkam, Surrey, U.K.) and observed via bright field illumination with a Leitz Diaplan

microscope (Germany). The sample was heated from 20 °C to 95 °C at 5 °C min^{-1} and a series of images were captured at different temperatures by a digital camera.

As for the acquisition of fluorescent images, whole psyllium husk powder was dispersed in saturated methyl blue and hydrated for 1 hour. Half of the dispersion was heated in a boiling water bath for 20 minutes followed by 1 hour cooling at room temperature. Then the heated and unheated samples were scanned by a fluorescence microscope (Evos FL, Waltham, US) equipped with a DAPI (357/44 - 447/60 nm) light cube. The heated psyllium husk powder fractions (collected after DSC traces) were stained with saturated methyl blue and scanned by the fluorescence microscope.

3. Results

3.1. Properties of whole psyllium husk powder dispersions

The moisture content, protein content, ash content and lipid content of psyllium husk powder were 7.23±0.03%, 3.40 ±0.03%, 2.89±0.01% and 3.30±0.30% respectively. The monosaccharide composition of psyllium husk powder includes 22.68±0.51%, arabinose, 3.32±0.12% galactose, 3.99±0.11% glucose and 55.38±0.98% xylose with total sugar of 85.36%. The results of chemical and monosaccharide composition analysis can be seen to be similar to Guo et al. (2008). The major monosaccharide components are arabinose and xylose. However, the contents of protein and lipid are slightly higher, which possibly indicates contamination during husking and milling processing from the endosperm.

The rheological properties of whole husk powder dispersion were measured by frequency sweep tests and temperature sweep tests (Figure 1). A freshly prepared suspension shows a gel-like property at room temperature as G’ is higher than G’’ (Figure 1a). The ‘gel’ melted during heating as both G’ and G’’ decreased whereas upon cooling a stronger ‘gel’ is formed, with G’ being much greater than G’’. Upon reheating and cooling this gel-like rheological property appears to be thermoreversible.

To understand the structure better, a frequency sweep test was performed on freshly prepared, heated (at 98 °C), and cooled psyllium husk powder dispersions and mechanical spectra are shown in Figure 1b**.** Both freshly prepared and cooled psyllium husk powder dispersions showed that G’ were higher than G’’ in the measurable frequency range and both moduli

show dependence on frequency. The logarithmic values of complex viscosity (η*) decreased linearly with that of frequency (ω) with slopes of -0.67 and -0.86 for freshly prepared and cooled psyllium husk powder dispersions respectively. The latter one is consistent with the results from Haque et al. (1993) on alkaline extracted psyllium husk dispersion, in which they suggested a similarity with xanthan showing 'weak gel' network. As for the freshly prepared dispersion, η* showed less dependence on ω, while G' and G'' were more frequency-dependent. However, the thermal property of the melting of dispersion was evaluated by DSC with the same temperature profile as the temperature sweep tests performed by rheometer (data not shown) and no thermal peaks were identified and the heat flow in the two cycles superimpose each other. This is in agreement with recent work by Yu et al. (2017) who described psyllium husk gels as 'physical gels'. Additionally, the T2 spectra of unheated and heated psyllium husk powder dispersions did not show any significant difference with a value of 977 ms for the dominant peak, which is assigned to water protons. It suggested that heat treatment does not influence water mobility in husk powder dispersions. Therefore, it is implausible that the three-dimensional network formation which occurs during conventional gelation cannot explain the significant rheological difference before and after heating.

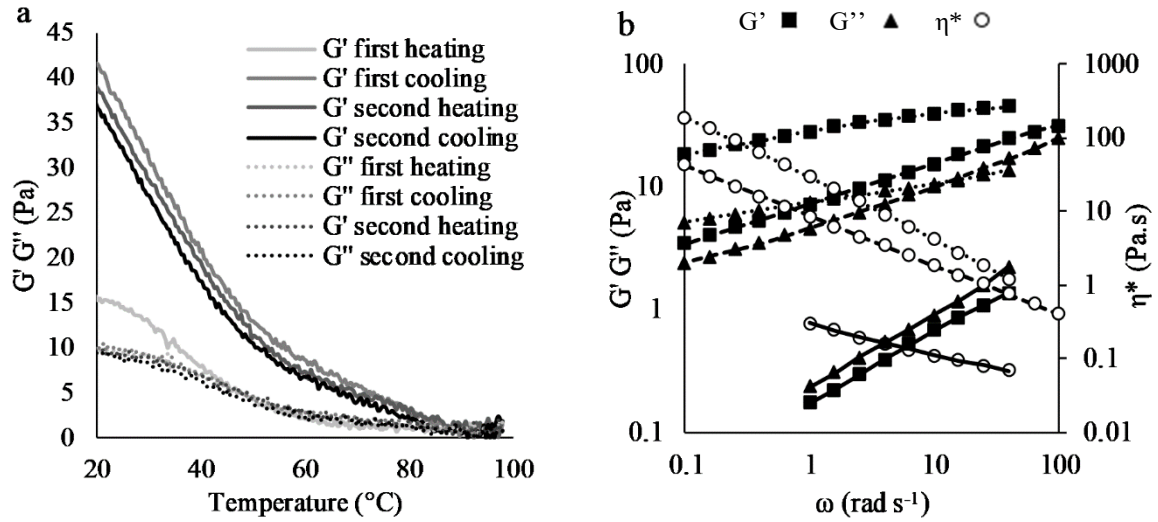

Figure 1. Storage and loss moduli (G' and G'') of 1.64% (w/w) psyllium husk powder dispersion over temperature changes (a) with a heating rate of 1 °C min-1, frequency of 10 rad s-1, and 0.02% strain. Mechanical spectra (b) of 1.64% husk powder dispersion at 20 °C before heating (– – –), at 98 °C (——), and after being heated at 20 °C (·····). The applied strain was 0.8% for tests at 20 °C and 2% for tests at 98 °C.

The mechanical spectrum of psyllium husk powder dispersion at 98 °C (Figure 1b) shows G'' slightly higher than G' with pronounced frequency dependence. It suggests melting of structure. The spectrum was found to be similar to Haque et al. (1993) who suggested that the melting has not been completed at, in their case, 91 °C, showing a residual gel-like character. Therefore, a possible interpretation of this data is that the weak interactions or bonds between molecules were disturbed by heating, therefore, the samples showed slightly more fluid-like property. Guo et al. (2009) described this 'melting' as a continuous and long procedure rather than a sharp melting period, evidenced by no change in enthalpy when analysed by DSC. Indeed Guo et al. (2009) also found their heat up and cooling profiles to be superimposable, without full melting of their gel structures up to 85°C.

To visualise the effect of heating psyllium husk dispersions, a hydrated husk particle was focused on under a light microscope equipped with a hot stage. The images obtained at 20 °C, 95 °C and 20 °C after cooled back are shown in Figure 2a. When the psyllium husk powder was hydrated, it swelled and formed a gel phase surrounding an insoluble core (visible under polarised light, image not shown) which is thought to be epidermis of the seeds. During heating from 20 °C to 95 °C, the gel phase gradually expanded and disappeared which did not recover after cooling back to room temperature. Only partial disappearance of this phase was observed and the remaining part was associated with the insoluble core which suggests that the gel phase contain different heteroxylan with different responses to temperature. Yu et al. (2017) identified three distinct mucilage layers of hydrated whole psyllium seed dominated by different arabinoxylans with different molecular conformation and rheological properties. To further visualise the psyllium husk powder dispersion, heated and unheated samples were stained by methyl blue and illuminated by fluorescent light (Figure 2b). The majority of psyllium husk polysaccharides are not water-soluble as clear hydrated particles were seen. Intact hydrated psyllium husk particles are observed in the left image though slight fibrous structures exist between the particles. At the concentration of 1.64% (w/w), these particles can be closely packed. Therefore, the freshly prepared psyllium husk dispersion can be described as concentrated suspension of gel particles and its rheological properties can be ascribed to the viscoelastic properties of the particles and physical contacts and frictions between them. However, after heat treatment, a fibrous structure with cloudy areas dominated the microstructure, which might play the role of junction zone formation and responsible for the thermoreversible gel-like properties.

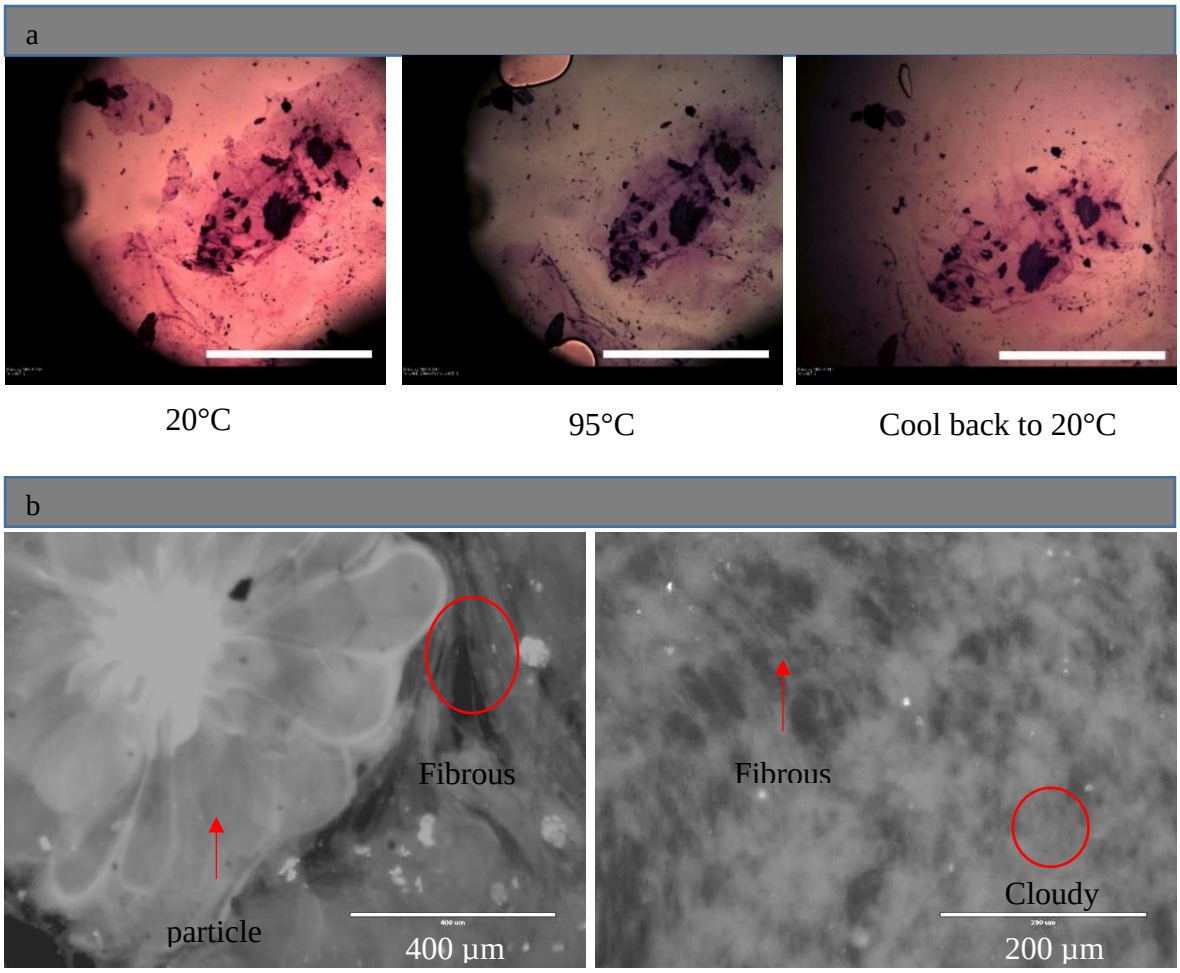

261

262 Figure 2. Bright field illumination of hydrated psyllium husk particle at different temperatures (a).
263 The sample was stained by toluidine blue and scanned by light microscope. Scale bar is 1 mm.
264 Fluorescent images of 1.64% psyllium husk powder dispersion (b) before (left) and after (right) heat
265 treatment in boiling water bath.

266 Table 1. Yields and A/X ratios of psyllium husk powder fractions

	Yield (%)	A/X ratio by		
		monosaccharide analysis	2^{nd}-derivative FTIR spectra peak 1/peak 2	^{13}C-NMR spectra $peak_{64}/peak_{66.3}$
F20	27.65	0.298±0.009	0.737	0.684
F40	19.05	0.305±0.006	0.884	0.919
F60	24.22	0.322±0.005	0.893	1.007
F80	8.96	0.363±0.010	1.63	1.497
F100	1.57	1.979±0.064	9.211	
Residue	13.66	10.048±2.348		
	95.11 (total yield)	0.417±0.002 (whole husk powder)	0.923 (whole husk powder)	0.385 (whole husk powder)

Fractionation of psyllium husk polysaccharides with water at different temperatures and alkaline were explored by Guo et al. (2008) and the fractions showed differences at the molecular level. Yu et al. (2017) discovered a formation of three layers of mucilage when the whole seeds were hydrated which can be extracted by cold water, warm water (65 °C), and alkaline. Based on the different rheological responses to temperature, the sequential fractionation of psyllium husk dispersion at four different temperatures has been explored.

3.2. Rheological properties

The water dispersion of psyllium husk powder was fractionated at different temperatures and four fractions were characterised by small amplitude oscillatory shear tests. Amplitude sweep spectra of these four fractions are shown in Figure 3a. All four fractions have a similar length of LVE regions. Interestingly, they showed G'' peaks before structure breakdown (final sharp decrease at high strain) which were more pronounced in F40, F60 and F80. This phenomenon is usually observed in concentrated dispersions and cross-linked polymers due to a significantly large amount of deformation energy released. Therefore, F20 is significantly different from other fractions at either the molecular level or in microstructures where there might be less or weaker molecular interactions or associations, or the molecular associates are less rigid.

Frequency sweep tests were performed on unheated and heated F20, F40, F60 and F80 at 20 °C. They were then tested at corresponding fractionating temperatures i.e. 20 °C, 40 °C, 60 °C and 80 °C respectively. The mechanical spectra are shown in Figure 3b, c, d and e. All fractions showed that G' is higher than G'' before and after heat treatment suggesting gel-like properties. However, only F20 show difference before and after heat treatment while others showed overlapping spectra. F80 showed slightly lower moduli after heat treatment, possibly, because of slight molecule degradation at high temperature or syneresis. Interestingly, all fractions displayed G' slightly higher than G'' at their individual fractionating temperatures which indicates that the fractionation did not happen in a solution state, instead, fractions tend to be rheologically dispersable at their fractionating temperature. Their rheological properties and extractability might be concentration and time dependent. Comparing all fractions, high temperature fractions show higher moduli and less dependence on frequency (F60 and F80 were similar) suggesting that high temperature fractions have stronger gel properties.

Similarly, as shown in Figure 6e, F20 and F40 did not withstand their own weights when placed upside down but F60 and F80 stayed on the bottom of the bottles.

The rheological responses were monitored during both heating and cooling, as shown in Figure 4. The storage moduli of F20 during the first heating was lower than cooling and the second heating and cooling cycle which was in agreement with mechanical spectra (Figure 3b, c, d and e), that heat treatment only influences F20. Apart from first heating for F20, other G' traces of all other fractions almost superimposed although there is a slight decrease during the second heating/cooling cycle, especially F80 possibly due to syneresis or high temperature-induced molecular degradation. Reversible rheological behaviour without hysteresis over temperature changes has also been reported previously on both whole psyllium husk extracts and fractionated samples (Guo et al., 2009; Haque et al., 1993). It is also noticed that the G' decrease during heating and G' increase during cooling were separated into three parts during which G' changed at different rates with a certain linear relationship with temperature when plotted in linear/linear scales. The rate of G' change during low and high temperatures was greater than that during the intermediate temperature range, which was also highlighted by Haque et al. (1993). They ascribed it to conformational transitions where coils are obtained at high temperature due to loss of conformational order. To further understand the difference between the four fractions, the data from the second heating were used to calculate the points where G' values changed decreasing rates as shown in Figure 4. The calculation was performed by defining upward and downward inflexions with 5% bandwidth. The second inflection points of F60 and F80 could not be calculated with these parameters though they are visually observable. The main discrepancy is that the first inflection points increased to a higher temperature in the order of F20 < F40 < F80 < F60 with 10°C difference. However, the positions of second infection points, which is likely due to loss of conformation order as suggested by Haque et al. (1993), happen at similar temperature (65 to 70 °C) over four fractions with similar and low G' values. The G' values decrease to almost zero at the end of heating (>88°C) indicating a high degree of melting of the structure. Weak interactions might exist which can only recover slowly.

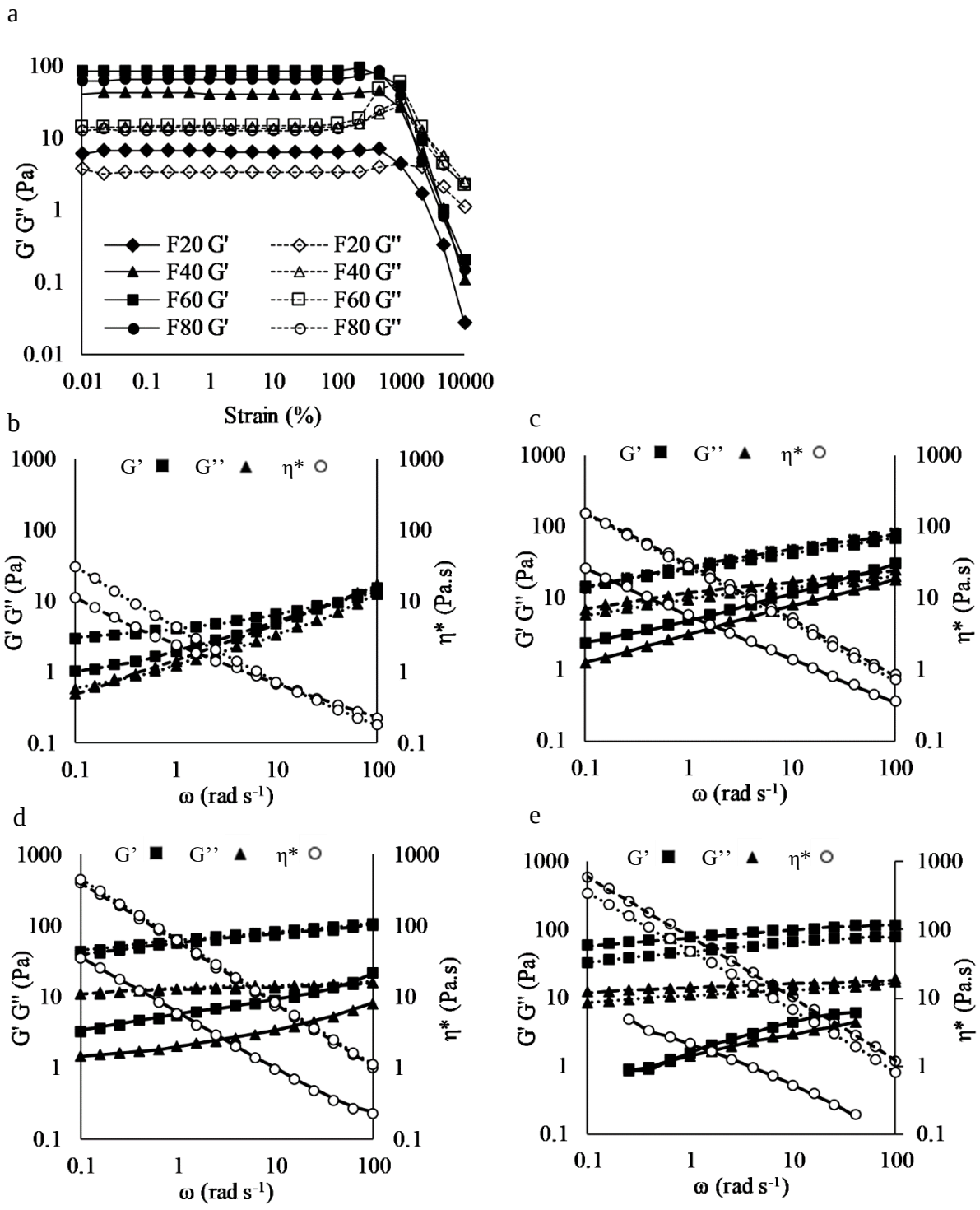

Figure 3. Amplitude sweep data of 1.64% F20, F40, F60 and F80 at 20 °C (a). Mechanical spectra of 1.64% F20 (b), F40 (c), F60 (d), and F80 (e). To obtain mechanical spectra, samples were tested at 20 °C before (– – –) and after (·····) heat treatment (98°C). F40, F60, and F80 were also tested at their fractionating temperatures (40 °C, 60 °C, and 80 °C individually) (——) which is different from 20 °C.

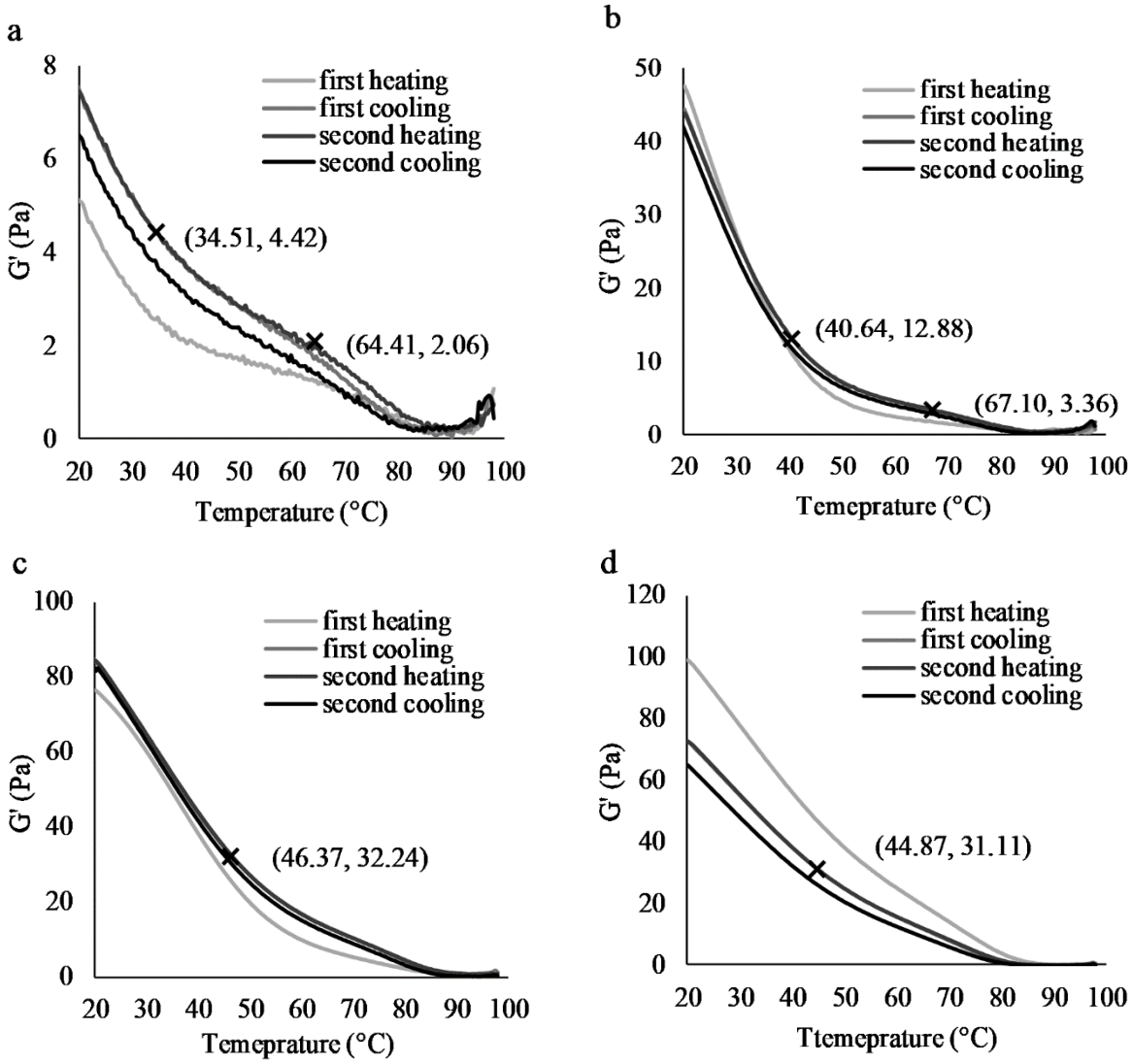

331

332 Figure 4. Storage moduli G' of 1.64% F20 (a), F40 (b), F60 (c), and F80 (d) over two cycles of
333 heating and cooling. Changes of melting speeds are shown as a cross (inflection point) on the graphs
334 which were calculated based on the second heating. Mathematical determination of the upward and
335 downward inflection points was performed on linear/linear scales with a bandwidth of 5%.

336 Table 2. Shifting factors (a) of angular frequency to obtain mater curves shown in Figure 5.

Measurement temperature °C	F20	F40	F60	F80
20	1	1	1	1
30	1.236E-01	7.159E-02	9.485E-02	8.387E-02
40	1.112E-02	4.655E-03	8.094E-03	6.299E-03
50	1.007E-03	3.329E-04	3.688E-04	2.426E-04
60	1.025E-04	2.553E-05	2.107E-05	1.549E-05
70	5.833E-06	1.183E-06	8.334E-07	5.527E-07
80	1.687E-07	3.086E-08	1.577E-08	8.665E-09

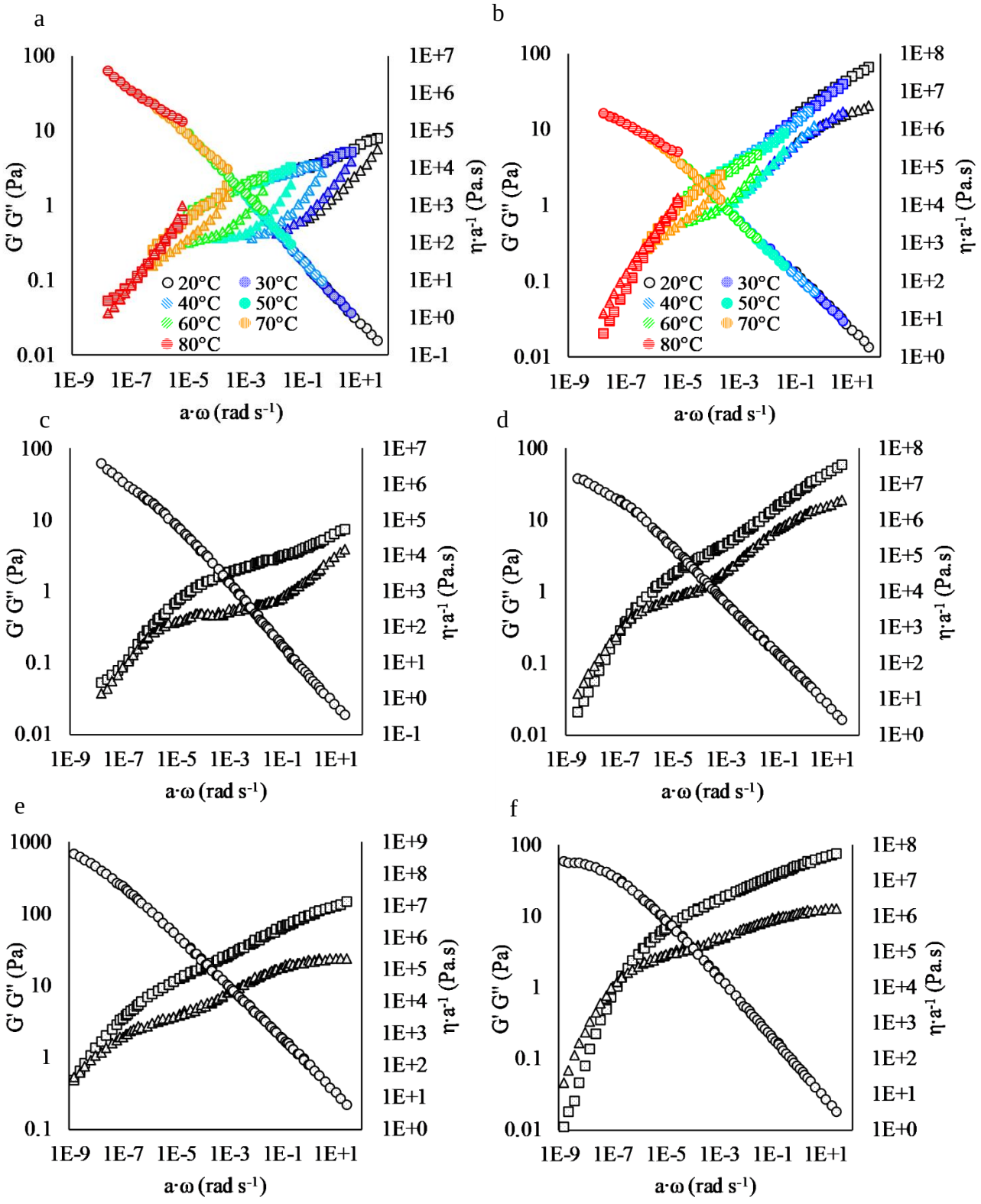

Figure 5. TTS of F20 (a) and F40 (b) after angular frequencies shifted and master curves of F20 (c) and F40 (d) with G'' smoothed as well as master curves of F60 (e) and F80 (f) without smoothing required (G', square; G'' triangle; $\eta^* a^{-1}$, circle). The concentration was 1.64% and the reference temperature is 20 °C. a is the shifting factor of angular frequency as listed in Table 2.

Similar to the dispersion of whole psyllium husk powder, no thermal peak was observed on DSC traces (data not shown). The assumption was therefore made that psyllium and fractions are thermo-rheologically simple materials and an attempt was made to perform TTS to further study the gelling properties (Figure 5). Frequency sweep tests were performed at different temperatures between 20 to 80 °C. The mechanical spectra measured at the same temperature were obtained with high reproducibility regardless of the temperature history they experienced which further support the reversible rheological behaviour observed in temperature sweep tests. The mechanical spectra at different temperatures were shifted to obtain master curves and the shifting factors (a) are shown in Table 2. However, the loss moduli of F20 and F40 (Figure 5a and b) were less well fitted and must be smoothed to generate master curves. The lack of superposition is caused by immiscibility, multiphase and semicrystalline formation with morphological changes (Nickerson, Paulson & Speers, 2004). Hence, molecular association or/and microstructural heterogeneity might exist in F20 and F40. As shown in Table 2, the shifting factors of high temperature fractions were lower which is reflected in master curves, as that high temperature fractions are slightly more shifted to the left. More evidently, F60 has a lower relaxation frequency (G'-G'' crossover frequency), i.e. longer relaxation time, compared to other fractions, which suggests longer or more branched molecules which is able to flow in a range of slow motion. Another interesting point is that, except for F20, the complex viscosity (η^*) of all other three fractions showed a tendency to reach a plateau of zero shear viscosity (η_0^*) which indicates the possibility that these polysaccharides behave like entangled polymers in a solution state. More interestingly, Yu et al. (2019) addressed structure similarity between gel state and solution state. The value of η_0^* of F60 tends to be the highest which also suggest a higher molecular weight.

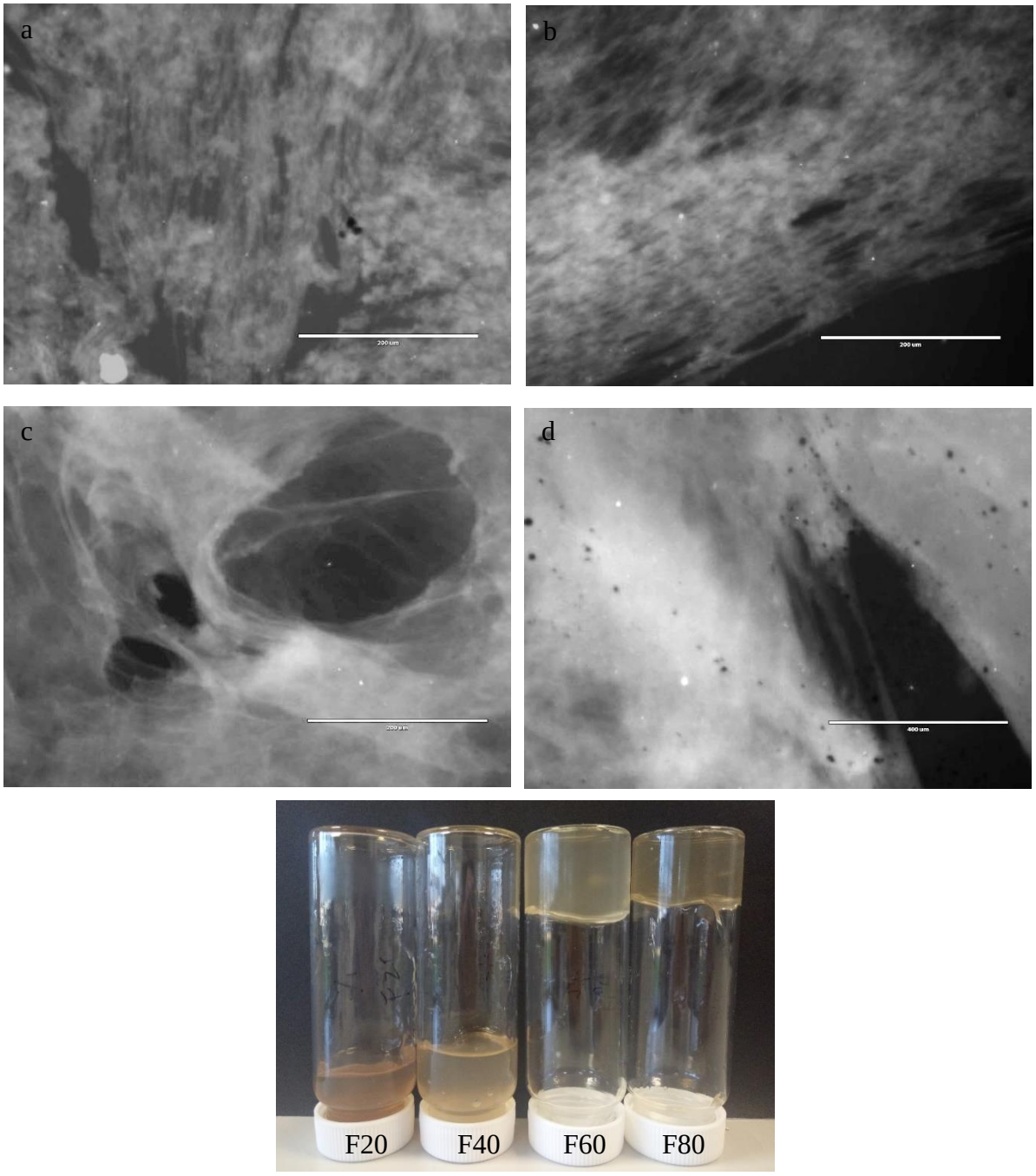

366

367 Figure 6. Fluorescent images of 1.64% heated F20 (a), F40 (b), F60 (c), F80 (d) stained with methyl
368 blue emitted by DAPI light and four fractions placed upside down (e).

369 **3.3. Microstructure of psyllium husk heteroxylan fractions**

370 Fluorescent images of heated fractions are shown in Figure 6. F20 and F40 showed fibrous
371 aggregates and more heterogeneous structures which are in agreement with the lack of fit of
372 G'' to obtain master curves of these two fractions in the TTS experiment. Nevertheless, the
373 structures of F60 and F80 are much finer. These structural differences are also reflected from

the decrease in turbidity from F20 to F80 (Figure 6e). The fibrous gel structure of psyllium husk dispersion has been also reported by Haque et al. (1993) and Guo et al. (2009) who investigated psyllium husk extracted by 2.5 M NaOH and 0.5 M NaOH, respectively. Compared to the image of heated whole psyllium dispersion (Figure 2b), it can be speculated that the fibrous strands are mainly low temperature fractions while the cloudy parts are high temperature fractions. It is worth mentioning that the heated whole psyllium husk dispersion is quite flexible and stretchable which forms stable bubbles easily as observed during experiment operations (data not shown). Such structure, i.e. strands linked by cloudy areas as 'junction zones', might be the foundation of the weak gel property and flexibility.

3.4. Chemical analysis of heteroxylans

3.4.1. Monosaccharide analysis

Arabinose to xylose (A/X) ratio (Table 1) was first considered and calculated based on the results of monosaccharide analysis. The whole psyllium husk powder sample showed an A/X ratio of 0.417 which is similar to the results from Van Craeyveld et al. (2009). A/X ratio increased in higher temperature fractions and F100 and residue show a ratio higher than 1. For most cereal arabinoxylans with simpler molecular structures, water solubility and extractability increase with higher A/X ratios since arabinose sidechains interfere the packing of xylan backbones (Andrewartha, Phillips & Stone, 1979; Izydorczyk, Macri & MacGregor, 1998; Mandalari et al., 2005; Zhang, Smith & Li, 2014). However, the data in Table 1 show that heteroxylan from psyllium husk with higher A/X ratio is harder to be extracted by water and requires higher temperatures. Therefore, the extractability and fractionation of psyllium husk heteroxylan must be influenced by other factors rather than solubility which is decided by backbone packing. In fact, as described in section 3.2, each fraction is rheologically dispersable at their fractionating temperature. In addition, the A/X ratios of whole psyllium husk and extractable fractions are generally lower than the heteroxylan or, more specifically, arabinoxylan from other cereals like wheat flour (0.5 – 0.8) (Cleemput, Roels, Van Oort, Grobet & Delcour, 1993; Izydorczyk, Biliaderis & Bushuk, 1991), wheat bran (0.5 - 1) (Aguedo, Fougnies, Dermience & Richel, 2014; Zhou et al., 2010), maize bran (Rose & Inglett, 2010), rye flour (1), rye bran (0.74) (Delcour, Vanhamel & De Geest, 1989), and non-waxy rice (0.7 – 1.2) (Lai, Lu, He & Chen, 2007). However, it has been evidenced that the heteroxylan from psyllium husk is highly branched (Fischer et al., 2004; Guo et al., 2008; Yu

et al., 2017). Hence, there should be a larger amount of xylose units in sidechains, especially in low temperature fractions which show lower A/X ratio.

3.4.2. FTIR spectroscopy

Full FTIR spectra and 2nd derivative spectra of whole psyllium husk powder and fractions are shown in Figure 7. The full spectra showed broad absorption peaks from approx. 3660 to 2990 cm^{-1} of O-H stretching vibrations and peaks of C-H stretching at 2924 and 2855 cm^{-1}. The peak of CO_2 absorption was seen at 2360 cm^{-1}. The peak at 1732 cm^{-1} was assigned to C=O stretching in the carboxyl group of uronic acid (Marchessault & Liang, 1962). It can be seen that F20 showed a slightly higher peak of uronic acid which is in agreement with Guo et al. (2008) that the fractions with higher uronic acid content are cold water-extractable. The peak at 1146/1162 cm^{-1} was assigned to C-O-C vibration of glycosidic bonds. The typical peak profile of arabinoglucuronoxylan due to ring vibrations, C-OH stretching vibrations of side groups, and C-O-C glycosidic bond vibration were observed showing peaks at 1162/1152, 1037/1027 cm^{-1} (Kacurakova, Capek, Sasinkova, Wellner & Ebringerova, 2000). Although the peaks at 1109 and 1070 cm^{-1} were not shown compared to the observation by Kacurakova et al. (2000), a shoulder at this range was seen. In addition, anomers of pyranose and furanose can be differentiated in the range of 900 to 800 cm^{-1} (Kacurakova et al., 2000; Mathlouthi & Koenig, 1987; Zhbankov, Andrianov & Marchewka, 1997). As shown in Figure 7a and the insert highlighting the range from 930 to 780 cm^{-1}, peaks were observed at 895 cm^{-1} assigned to β-linkage of pyranoses in all spectra with obvious shoulders at 866 cm^{-1} assigned to α-linkage of furanose in residue and F100. The shoulder was also shown in F40, F60 and F80 with similar intensity but less pronounced in F20. It has been evidenced that the psyllium polysaccharide is constituted by β-xylose in pyranose form in the backbone and both α-arabinose in furanose form and β-xylose in sidechains substituting on C-3 or/and C-2 (Edwards et al., 2003; Fischer et al., 2004; Guo et al., 2008; Yu et al., 2017). Therefore, the observation suggests that residue and F100 are heavily substituted by arabinose followed by F40, F60 and F80 while F20 is less branched by arabinose.

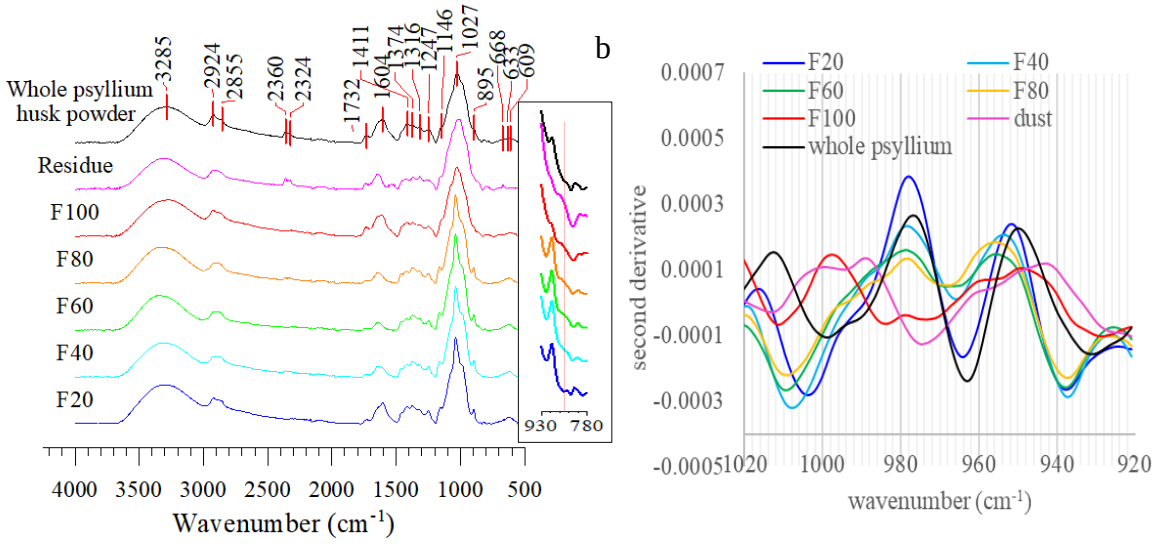

Figure 7. FTIR spectra of whole psyllium husk powder and fractions (a) and 2nd derivative (multiplied by -1) of the region from 1020 to 920 cm^{-1} (b). The insert shows details from 930 to 780 cm^{-1} highlighting the shoulder at 866 cm^{-1} guided by a red line.

Second-derivative spectra of arabinoxylan in the range from 1020 to 920 cm^{-1} reflect A/X ratio and substitution positions on xylan backbones (Robert, Marquis, Barron, Guillon & Saulnier, 2005). The second derivative spectra of whole psyllium, F20, F40, F60 and F80 (Figure 7b) show two peaks at approximately 978 (peak 2) and 955 (peak 1) cm^{-1} and the height ratio of these two peaks was calculated and shown in Table 1. From F20 to F100, peak 1/peak 2 increased which is another evidence of the increase of A/X ratio (Robert et al., 2005). A peak appeared at 943 cm^{-1} in the spectra of F100 and residue suggest a possible increase of C-2 substitution (Robert et al., 2005).

3.4.3. ^{13}C solid-state NMR spectroscopy

Whole psyllium husk powder and freeze-dried factions were subjected to CPMAS NMR spectroscopy analysis shown in Figure 8. Except for residue, all other samples show a similar peak at 104 ppm which is a merging for C1 of arabinose, xylose and other monosaccharide residues. Therefore, A/X ratio cannot be calculated by integrating this peak as described by Rondeau-Mouro, Ying, Ruellet and Saulnier (2011). However, some differences were noticed in the range from 95 to 68 ppm which are assigned to C2 to C4 of polysaccharides. Because substitution by either neighbouring monosaccharide residue in the backbone or by sidechains leads to downfield shift, a detailed evaluation of this range can help to differentiate molecular conformation in terms of branching and glycosidic bonds. All spectra showed peaks or

shoulder at 82 ppm assigned to substituted C2 and C3 while unsubstituted C2 and C3 contribute to peaks at 75 ppm with a shoulder at 76 ppm assigned to substituted C4. A discernible peak of unsubstituted C4 was at 70 ppm. The high temperature fractions revealed a lower intensity of unsubstituted C2 and C3 which indicates that high temperature fractions might be heavily branched on C2 and C3 of the xylan backbone. An obvious increase in peak intensity of unsubstituted C4 was noticed in lower temperature fractions. Arabinose units are only linked via 1→3 linkages (Fischer et al., 2004; Guo et al., 2008), therefore the difference is mainly attributed to linkages of xylose residue and there might be more unsubstituted C4 of xylose units in lower temperature fractions especially F20. There are two possibilities: Firstly that low temperature fractions have more branching xylose as monosaccharide substitutes or sidechains containing xylose units. These xylose units can be terminal xylose in sidechains. They can also be 1→3 linked xylose in the middle position of trisaccharides sidechains (Fischer et al., 2004). Therefore, the unsubstituted C4 could belong to either terminal xylose or xylose in the middle position of sidechains. Another possibility is that there are more 1→3 linkages in the xylan backbones of low temperature fractions (Guo et al., 2008; Haque et al., 1993; Kennedy, Sandhu & Southgate, 1979; Sandhu et al., 1981). Haque et al. (1993) and Sandhu et al. (1981) presumed alternating 1→3 and 1→4 linkage arrangement and 1→3 linkages in the backbone lead to conformational changes of the macromolecules.

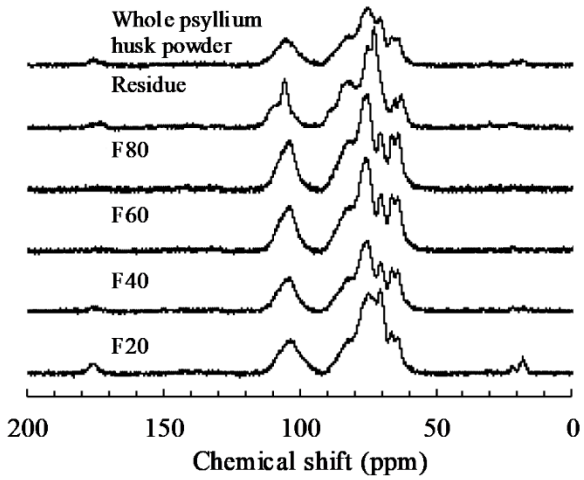

Figure 8. Solid state ^{13}C NMR spectra (normalised to the integral signal) of F20, F40, F60, F80, residue and whole psyllium husk powder.

Although C1 peaks were not separated, C5 of xylose (66 ppm) and arabinose (64.0 ppm) residue were clearly resolved on the spectra. Signals from C5 of arabinose and xylose were

integrated and the ratio was calculated to estimate A/X ratio as shown in Table 1. The results were comparable to the ratios calculated from FTIR 2nd-derivative spectra but both are higher than the results of monosaccharide analysis. Correction must be applied as the calculation are based on the abundance of carbon atom but it further evidenced that high temperature fractions contain more arabinose units.

Residue was distinct from others with distinguishable C1 peaks at 109.4 ppm and 105.4 ppm. It also showed a signal at 88.4 ppm as a shoulder which is related to C4 of crystalline cellulose (Atalla & Vanderhart, 1984; Wickholm, Larsson & Iversen, 1998). The shoulder assigned to substituted C4 of xylan is absent compared to other fractions but residue showed a sharp peak at 72.6 ppm. It is difficult to assign this peak but, considering the high amount of arabinose in residue, it might be assigned to C2 of arabinose (Fischer et al., 2004; Palaniappan, Yuvaraj, Sonaimuthu & Antony, 2017). However, it might be related to C2/C5 of cellulose I_{α} (Kono et al., 2002). Therefore, the presence of arabinan and cellulose in crystalline form can be speculated.

The spectrum of whole psyllium show three small peaks at 175, 22 and 18 ppm, which suggests the existence of small amounts of pectin and protein (Alba et al., 2018; Foster, Ablett, McCann & Gidley, 1996). These three peaks are also observed in the spectra of F20 and residue, therefore these pectin or/and protein are either cold water extractable or not extractable.

4. Discussion: Molecular structure and conformation and gel forming mechanism

We have demonstrated that four psyllium fractions show distinct rheological properties microstructures. We also evidenced that they are different in sidechain composition and substitution degree of sidechains. Sidechains of polysaccharides have significant and complex impacts on the molecular conformation and behaviours in solutions. As mentioned in section 3.4.1, solubility can be increased and chain association can be interfered by higher degrees of substitution as exampled by cereal arabinoxylan and cellulose ethers. However, psyllium husk heteroxylans are distinct from other cereal arabinoxylans as they are heavily substituted but with lower A/X ratios (xylose units in sidechains). Psyllium heteroxylans, at least the majority of them, are insoluble in water and show gel-like property upon hydration. There are no direct evidence or literature details the molecular structures or conformations of

psyllium husk heteroxylans. However, sidechain compositions and spatial arrangements are likely to play a critical role in diversifying the rheological properties of these macromolecules. We propose two hypotheses to understand the distinct rheological behaviours. One focus on chemical and structural properties of the heteroxylan molecules and the other one bases on hierarchical molecular conformations.

The conformation of dry arabinoxylan from rice endosperm cell wall is an extended, left-handed, three-fold helix (Yui, Imada, Shibuya & Ogawa, 1995). However, the conformation of soluble arabinoxylan from wheat in solution is proposed to be semi-flexible random coils (Dervilly-Pinel, Thibault & Saulnier, 2001). Haque et al. (1993) proposed that psyllium husk arabinoxylan adopts conformation of three-fold twisted ribbon based on work by Nieduszynski and Marchessault (1972), that hydrated xylan forms anti-parallel three-fold helical molecule chains with water columns forming hydrogen bonds between neighbouring chains. The water molecules between xylan chains can be replaced by monosaccharide substitution on O-2 and/or O-3 (Haque et al., 1993). It is highly possible that this model by Haque et al. (1993) can describe the case of low temperature fraction which is possibly less substituted or substituted with mono-units of xylose. However, the existence of other factors, e.g. longer sidechains or 1→3 linkages in backbone etc., might disturb this molecular association. Therefore, the heteroxylan molecules in low temperature fractions partially associate and then form 'weak gel' with fibrous structure (figure 6) characterised as ordered and rigid chains cross-linked by weak junction zones as suggested by Haque et al. (1993). The molecular association is evidenced by rheological behaviours (amplitude sweep tests and TTS) as described in section 3.2.

On the other hand, as shown in Figure 6, the structure of high temperature fractions are finer which indicates that the extensive inter-chain association is restricted. As described earlier, the high temperature fractions are substituted to a higher degree than low temperature fractions, with higher A/X ratio. In addition, there are long sidechains composed of 2 or more arabinose or/and xylose (Yu et al., 2017) such as Ara-α-(1→3)-Xyl-β-(1→3)-Ara reported by (Fischer et al., 2004), which do not fit into the packing model of xylan. Hence, chain association in high temperature fractions is prohibited. Therefore, the gel structure is possibly maintained by hydrogen bonds between sidechains as advised by Yu et al. (2019) who suggested 'physical gel' to describe this structure. The strength, amount, and

time/temperature-dependence formation of hydrogen bonds between sidechains could be dependent more on entropic favourability. Moreover, the high degree of sidechain substitution also increases chain rigidity sterically which might contributes to the stronger gel property, as shown in Figure 3b, c, d and e.

The psyllium fractions show three-step G' decrease during heating with two sharp and one intermediate slower decrease (Figure 4). Haque et al. (1993) assigned the differences to helical conformational transitions and loss of conformations transferring into coils. The initial sharp G' decrease is likely due to the temperature-dependent softening. The intermediate slower G' decrease and the decrease at higher temperature range might be assigned to conformational transitions of the helical molecules and the final transition into coils. The structural transition during heating and cooling of these heteroxylans are similar to xanthan which also undergoes helix-coil transition during heating (Norton, Goodall, Frangou, Morris & Rees, 1984). This three step softening and melting process is reversible as shown by its reversible rheological behaviour (Figure 4). The low temperature fractions finish the initial temperature-dependent softening at a slightly lower temperature but the high temperature fractions complete this process at a higher temperature. However, the conformational transitions and loss of ordered molecular conformation occur at similar temperature ranges for all four fractions which suggest similarities in their molecular structures and conformations. In addition, the initial heat treatment only increased the moduli of F20 (Figure 3 and Figure 4) suggesting that the heat treatment influences its molecular association which is, then, reversible during following heating-cooling cycles.

Another hypothesis could be made to describe the structures and conformations of psyllium husk heteroxylans based on Diener et al. (2019)'s hierarchical structure model for polysaccharides based on carrageenan that the primary linear structure forms single helices as secondary structure which further forms supercoiled helices (tertiary structure) and the quaternary structure includes intermolecular supercoiling. Being different from carrageenan, psyllium husk heteroxylans are heavily substituted by complex sidechains. Sidechains can be critical in determining the backbone conformation which is the case of 5-fold helical xanthan (Foster, 1992). The properties of sidechains can contribute significantly to the properties of polysaccharide which was well exampled by Abbaszadeh et al. (2015) that xanthan, which is acetylated and pyruvylated to different degrees, varies on shear rheology moduli and

conformational transition temperature. Psyllium husk heteroxylan, especially the low temperature fraction, could also form tertiary and quaternary supercoiling as molecular associations. However, ^{13}C NMR spectra show that high temperature fraction is highly substituted on C2 and C3 by, possibly, long sidechains, which influence the spatial arrangement and increase chain rigidity, which is shown as G' and G'' overshot in amplitude sweep tests and longer relaxation time reflected by TTS master curves. The increased rigidity is likely to interfere with the further formation of compact tertiary and quaternary structure in high temperature fractions. Based on Diener et al. (2019)'s model, the three-step G' decrease during heating and G' increase during cooling reflect initial temperature-dependent softening and stepwise melting and recovery of the hierarchical structure. F20 is the only fraction showing a more gel-like property after heat treatment, which indicates conformational difference caused by temperature changes. Other higher temperature fractions and F20 in the following heating and cooling cycles show reversible conformational transitions.

The possibility must be taken into consideration that the sidechain substitution of psyllium husk heteroxylans could be complicated. Each fraction could contain different molecules with different rheological properties. Classification of these heteroxylans and a specific and purifying fractionation or extraction process might be problematic. In addition, blockiness is widely found in nature that, for example, blocky distribution of sidechains influences the sidechain-dominated properties of polysaccharides, such as de-esterified pectin and cellulose (Ström et al., 2007; Sullo, Wang, Koschella, Heinze & Foster, 2013). blocky distribution of motifs with certain molecular, conformational or rheological characteristics could also exist in psyllium heteroxylans which lead to further complexity.

5. Conclusion

It has been noticed that hydrated whole psyllium husk powder shows a gel-like property which melts during heating while forming a stronger gel during cooling where a combined fibrous and cloudy structure was observed. It then melts and recovers reversibly during following heating and cooling. A simple sequential fractionation of psyllium husk heteroxylans was performed. The fractions are rheological dispersible instead of being soluble at their corresponding fractionating temperatures. High temperature fractions show stronger gel-like property. The four fractions show reversible three step softening and melting process during heating. F60 is distinct from other fractions as 1) the first sharp G' decrease

stopped at a higher temperature even than F80 (Figure 4), 2) it showed lower relaxation frequency which is longer relaxation time (Figure 5), 3) F60 showed highest η_0* according to the tendency (Figure 5). The reason is unknown, but it might be due to a higher degree of polymerisation, longer sidechains, or/and heavy substitution by sidechains, which increase chain rigidity. The high temperature fractions showed slightly higher A/X ratio and, possibly, a higher degree of substitution. The differences between the composition of sidechains lead to different intermolecular association and rheological properties. Two hypotheses were proposed based on either chemical and structural properties or hierarchical molecular conformations. The first hypothesis applies Haque et al. (1993)'s model on low temperature fractions which support the molecular association as reflected in amplitude sweep tests, TTS and microstructures while 'physical gel' by Yu et al. (2019) might describe high temperature fractions. The second hypothesis is based on the hierarchical molecular conformations which can be influenced by sidechain compositions and spatial arrangements. The three step softening and melting might due to changes in helical conformation and transition into coils or to softening and melting of tertiary and quaternary conformations.

However, there is no comprehensive evidence describing the molecular structure and conformation of psyllium husk heteroxylan and further investigations on sidechain composition and distribution and molecular conformation are necessary. Additionally, further investigation focusing on F60 and comparison between this fraction with alkaline extractable fractions would be intriguing. Investigations on long-term behaviours, e.g. aggregation and syneresis, would be also important for a deeper understanding and further application of this material.

Acknowledgement

This work was supported by the University of Nottingham (Vice-Chancellor's Scholarship for Research Excellence (International)) and PepsiCo. The views and opinions expressed in this manuscript are those of the author and do not necessarily reflect the position or policy of PepsiCo. The authors would also like to thank Roger Ibbett for helping with monosaccharide analysis.

Reference

Abbaszadeh, A., Lad, M., Janin, M., Morris, G. A., MacNaughtan, W., Sworn, G. & Foster, T. J. (2015). A novel approach to the determination of the pyruvate and acetate distribution in xanthan. *Food Hydrocolloids, 44*, 162-171.

Aguedo, M., Fougnies, C., Dermience, M. & Richel, A. (2014). Extraction by three processes of arabinoxylans from wheat bran and characterization of the fractions obtained. *Carbohydrate Polymers, 105*, 317-324.

Alba, K., MacNaughtan, W., Laws, A. P., Foster, T. J., Campbell, G. M. & Kontogiorgos, V. (2018). Fractionation and characterisation of dietary fibre from blackcurrant pomace. *Food Hydrocolloids, 81*, 398-408.

Anderson, J. W., Allgood, L. D., Lawrence, A., Altringer, L. A., Jerdack, G. R., Hengehold, D. A. & Morel, J. G. (2000). Cholesterol-lowering effects of psyllium intake adjunctive to diet therapy in men and women with hypercholesterolemia: meta-analysis of 8 controlled trials. *The American Journal of Clinical Nutrition, 71*(2), 472-479.

Andrewartha, K. A., Phillips, D. R. & Stone, B. A. (1979). Solution properties of wheat-flour arabinoxylans and enzymically modified arabinoxylans. *Carbohydrate Research, 77*, 191-204.

Atalla, R. H. & Vanderhart, D. L. (1984). Native cellulose: A composite of two distinct crystalline forms. *Science, 223*(4633), 283-285.

Cappa, C., Lucisano, M. & Mariotti, M. (2013). Influence of psyllium, sugar beet fibre and water on gluten-free dough properties and bread quality. *Carbohydrate Polymers, 98*(2), 1657-1666.

Chavanpatil, M. D., Jain, P., Chaudhari, S., Shear, R. & Vavia, P. R. (2006). Novel sustained release, swellable and bioadhesive gastroretentive drug delivery system for ofloxacin. *International Journal of Pharmaceutics, 316*(1), 86-92.

Cheng, Z., Blackford, J., Wang, Q. & Yu, L. (2009). Acid treatment to improve psyllium functionality. *Journal of Functional Foods, 1*(1), 44-49.

Cleemput, G., Roels, S., Van Oort, M., Grobet, P. & Delcour, J. (1993). Heterogeneity in the structure of water-soluble arabinoxylans in European wheat flours of variable bread-making quality. *Cereal Chemistry, 70*, 324-324.

Delcour, J., Vanhamel, S. & De Geest, C. (1989). Physico-chemical and functional properties of rye nonstarch polysaccharides. I. Colorimetric analysis of pentosans and their relative monosaccharide compositions in fractionated (milled) rye products. *Cereal Chemistry, 66*(2), 107-111.

Dervilly-Pinel, G., Thibault, J.-F. & Saulnier, L. (2001). Experimental evidence for a semi-flexible conformation for arabinoxylans. *Carbohydrate Research, 330*(3), 365-372.

Diener, M., Adamcik, J., Sánchez-Ferrer, A., Jaedig, F., Schefer, L. & Mezzenga, R. (2019). Primary, secondary, tertiary and quaternary structure levels in linear polysaccharides: From random coil, to single helix to supramolecular assembly. *Biomacromolecules, 20*(4), 1731-1739.

Edwards, S., Chaplin, M. F., Blackwood, A. D. & Dettmar, P. W. (2003). Primary structure of arabinoxylans of ispaghula husk and wheat bran. *Proceedings of the Nutrition Society, 62*(1), 217-222.

Farahnaky, A., Askari, H., Majzoobi, M. & Mesbahi, G. (2010). The impact of concentration, temperature and pH on dynamic rheology of psyllium gels. *Journal of Food Engineering, 100*(2), 294-301.

Fischer, M. H., Yu, N. X., Gray, G. R., Ralph, J., Anderson, L. & Marlett, J. A. (2004). The gel-forming polysaccharide of psyllium husk (Plantago ovata Forsk). *Carbohydrate Research, 339*(11), 2009-2017.

Foster, T. J. (1992). *Conformation and properties of xanthan variants.* PhD thesis, Cranfield Institute of Technology, Silsoe College, Bedfordshire, UK.

Foster, T. J., Ablett, S., McCann, M. C. & Gidley, M. J. (1996). Mobility-resolved 13C-NMR spectroscopy of primary plant cell walls. *Biopolymers, 39*(1), 51-66.

Guo, Q., Cui, S. W., Wang, Q., Goff, H. D. & Smith, A. (2009). Microstructure and rheological properties of psyllium polysaccharide gel. *Food Hydrocolloids, 23*(6), 1542-1547.

Guo, Q., Cui, S. W., Wangb, Q. & Young, J. C. (2008). Fractionation and physicochemical characterization of psyllium gum. *Carbohydrate Polymers, 73*(1), 35-43.

Haque, A. & Morris, E. R. (1994). Combined use of ispaghula and HPMC to replace or augment gluten in breadmaking. *Food Research International, 27*(4), 379-393.

Haque, A., Richardson, R. K., Morris, E. R. & Dea, I. C. M. (1993). Xanthan-like weak gel rheology from dispersions of ispaghula seed husk. *Carbohydrate Polymers, 22*(4), 223-232.

Izydorczyk, M., Biliaderis, C. & Bushuk, W. (1991). Comparison of the structure and composition of water-soluble pentosans from different wheat varieties. *Cereal Chemistry, 68*(2), 139-144.

Izydorczyk, M. S., Macri, L. J. & MacGregor, A. W. (1998). Structure and physicochemical properties of barley non-starch polysaccharides—II. Alkaliextractable β-glucans and arabinoxylans. *Carbohydrate Polymers, 35*(3), 259-269.

Kacurakova, M., Capek, P., Sasinkova, V., Wellner, N. & Ebringerova, A. (2000). FT-IR study of plant cell wall model compounds: pectic polysaccharides and hemicelluloses. *Carbohydrate Polymers, 43*(2), 195-203.

Kennedy, J. F., Sandhu, J. S. & Southgate, D. A. T. (1979). Structural data for the carbohydrate of Ispaghula Husk ex *Plantago ovata* Forsk. *Carbohydrate Research, 75*, 265-274.

Kono, H., Yunoki, S., Shikano, T., Fujiwara, M., Erata, T. & Takai, M. (2002). CP/MAS ^{13}C NMR study of cellulose and cellulose derivatives. 1. Complete assignment of the CP/MAS ^{13}C NMR spectrum of the native cellulose. *Journal of the American Chemical Society, 124*(25), 7506-7511.

Lai, V. M. F., Lu, S., He, W. H. & Chen, H. H. (2007). Non-starch polysaccharide compositions of rice grains with respect to rice variety and degree of milling. *Food Chemistry, 101*(3), 1205-1210.

Laidlaw, R. A. & Percival, E. G. V. (1949). Studies on seed mucilages. Part III. Examination of a polysaccharide extracted from the seeds of Plantago ovata forsk. *Journal of the Chemical Society*, 1600-1607.

Madgulkar, A. R., Rao, M. R. P. & Warrier, D. (2015). Characterization of psyllium (plantago ovata) polysaccharide and its uses. In K. G. Ramawat & J.-M. Mérillon (Eds.), *Polysaccharides: Bioactivity and Biotechnology* (pp. 1-17). New York: Springer International Publishing.

Mancebo, C. M., San Miguel, M. Á., Martínez, M. M. & Gómez, M. (2015). Optimisation of rheological properties of gluten-free doughs with HPMC, psyllium and different levels of water. *Journal of Cereal Science, 61*, 8-15.

Mandalari, G., Faulds, C. B., Sancho, A. I., Saija, A., Bisignano, G., LoCurto, R. & Waldron, K. W. (2005). Fractionation and characterisation of arabinoxylans from brewers' spent grain and wheat bran. *Journal of Cereal Science, 42*(2), 205-212.

Marchessault, R. H. & Liang, C. Y. (1962). The infrared spectra of crystalline polysaccharides. VIII. Xylans. *Journal of Polymer Science, 59*(168), 357-378.

Mariotti, M., Lucisano, M., Pagani, M. A. & Ng, P. K. W. (2009). The role of corn starch, amaranth flour, pea isolate, and psyllium flour on the rheological properties and the ultrastructure of gluten-free doughs. *Food Research International, 42*(8), 963-975.

Marlett, J. & Fischer, M. (2005). Gel-forming polysaccharide from psyllium seed husks. WO2005116087A1.

Mathlouthi, M. & Koenig, J. L. (1987). Vibrational spectra of carbohydrates. In R. S. Tipson & D. Horton (Eds.), *Advances in Carbohydrate Chemistry and Biochemistry* (Vol. 44, pp. 7-89): Academic Press.

Nickerson, M. T., Paulson, A. T. & Speers, R. A. (2004). Time–temperature studies of gellan polysaccharide gelation in the presence of low, intermediate and high levels of co-solutes. *Food Hydrocolloids, 18*(5), 783-794.

Nieduszynski, I. A. & Marchessault, R. H. (1972). Structure of β,D(1->4')-xylan hydrate. *Biopolymers, 11*(7), 1335-1344.

Norton, I. T., Goodall, D. M., Frangou, S. A., Morris, E. R. & Rees, D. A. (1984). Mechanism and dynamics of conformational ordering in xanthan polysaccharide. *Journal of Molecular Biology, 175*(3), 371-394.

Palaniappan, A., Yuvaraj, S. S., Sonaimuthu, S. & Antony, U. (2017). Characterization of xylan from rice bran and finger millet seed coat for functional food applications. *Journal of Cereal Science, 75*, 296-305.

Rao, M. R. P., Warrier, D. U., Gaikwad, S. R. & Shevate, P. M. (2016). Phosphorylation of psyllium seed polysaccharide and its characterization. *International Journal of Biological Macromolecules, 85*, 317-326.

Robert, P., Marquis, M., Barron, C., Guillon, F. & Saulnier, L. (2005). FT-IR investigation of cell wall polysaccharides from cereal grains. Arabinoxylan infrared assignment. *Journal of Agricultural and Food Chemistry, 53*(18), 7014-7018.

Rondeau-Mouro, C., Ying, R., Ruellet, J. & Saulnier, L. (2011). Structure and organization within films of arabinoxylans extracted from wheat flour as revealed by various NMR spectroscopic methods. *Magnetic Resonance in Chemistry, 49*(S1), S85-S92.

Rose, D. J. & Inglett, G. E. (2010). Production of feruloylated arabinoxylo-oligosaccharides from maize (*Zea mays*) bran by microwave-assisted autohydrolysis. *Food Chemistry, 119*(4), 1613-1618.

Sandhu, J. S., Hudson, G. J. & Kennedy, J. F. (1981). The gel nature and structure of the carbohydrate of ispaghula husk ex Plantago ovata Forsk. *Carbohydrate Research, 93*(2), 247-259.

Singh, B. (2007). Psyllium as therapeutic and drug delivery agent. *International Journal of Pharmaceutics, 334*(1), 1-14.

Song, Y.-J., Sawamura, M., Ikeda, K., Igawa, S. & Yamori, Y. (2000). Soluble dietary fibre improves insulin sensitivity by increasing muscle glut-4 content in stroke-prone spontaneously hypertensive rats. *Clinical and Experimental Pharmacology and Physiology, 27*(1-2), 41-45.

Ström, A., Ribelles, P., Lundin, L., Norton, I., Morris, E. R. & Williams, M. A. K. (2007). Influence of pectin fine structure on the mechanical properties of calcium−pectin and acid−pectin gels. *Biomacromolecules, 8*(9), 2668-2674.

Sullo, A., Wang, Y., Koschella, A., Heinze, T. & Foster, T. J. (2013). Self-association of novel mixed 3-mono-O-alkyl cellulose: Effect of the hydrophobic moieties ratio. *Carbohydrate Polymers, 93*(2), 574-581.

Van Craeyveld, V., Delcour, J. A. & Courtin, C. M. (2009). Extractability and chemical and enzymic degradation of psyllium (Plantago ovata Forsk) seed husk arabinoxylans. *Food Chemistry, 112*(4), 812-819.

Wickholm, K., Larsson, P. T. & Iversen, T. (1998). Assignment of non-crystalline forms in cellulose I by CP/MAS 13C NMR spectroscopy. *Carbohydrate Research, 312*(3), 123-129.

Yu, L., Yakubov, G. E., Gilbert, E. P., Sewell, K., van de Meene, A. M. L. & Stokes, J. R. (2019). Multi-scale assembly of hydrogels formed by highly branched arabinoxylans from Plantago ovata seed mucilage studied by USANS/SANS and rheology. *Carbohydrate Polymers, 207*, 333-342.

Yu, L., Yakubov, G. E., Zeng, W., Xing, X., Stenson, J., Bulone, V. & Stokes, J. R. (2017). Multi-layer mucilage of Plantago ovata seeds: Rheological differences arise from variations in arabinoxylan side chains. *Carbohydrate Polymers, 165*, 132-141.

Yui, T., Imada, K., Shibuya, N. & Ogawa, K. (1995). Conformation of an arabinoxylan isolated from the rice endosperm cell wall by X-ray diffraction and a conformational analysis. *Bioscience, Biotechnology, and Biochemistry, 59*(6), 965-968.

Zhang, Z. X., Smith, C. & Li, W. L. (2014). Extraction and modification technology of arabinoxylans from cereal by-products: A critical review. *Food Research International, 65*, 423-436.

Zhbankov, R. G., Andrianov, V. M. & Marchewka, M. K. (1997). Fourier transform IR and Raman spectroscopy and structure of carbohydrates. *Journal of Molecular Structure, 437*, 637-654.

Zhou, S. M., Liu, X. Z., Guo, Y., Wang, Q. A., Peng, D. Y. & Cao, L. (2010). Comparison of the immunological activities of arabinoxylans from wheat bran with alkali and xylanase-aided extraction. *Carbohydrate Polymers, 81*(4), 784-789.